Acta Polytechnica CTU Proceedings **44**:5–12, 2023
https://doi.org/10.14311/APP.2023.44.0005

Published by the Czech Technical University in Prague

THERMOMECHANICAL CALCULATION WITHIN THE HERA PROGRAMME

Tereza Kinkorová

Czech Technical University in Prague, Faculty of Nuclear Sciences and Physical Engineering, Department of Nuclear Reactors, V Holešovičkách 2, 180 00 Prague 8, Czech Republic

correspondence: kinkoter@fjfi.cvut.cz

Abstract. HERA (High Burnup Experiments in Reactivity Initiated Accident) is one of the programmes which should replace closed Halden reactor. As the name implies HERA is focused on the tests simulated RIA (Reactivity Initiated Accident) and the aim of the programme is to investigate the performance and behaviour of high burnup fuel in RIA transients. The first phase of HERA programme consists of two steps which are the blind calculation of different RIA scenarios (different pulse width, enthalpy increase, hydrogen content and gap size) and in-reactor test with fresh fuel.

The set of thermomechanical calculation was performed with the FRAPTRAN computer code as part of the first phase of HERA. The influence of several parameters on the fuel behaviour was observed, the varying parameters were the pulse width, peak radial average enthalpy increase, hydrogen content and the hydrogen rim size and gap size. In addition, the effect of type and setting of boundary condition was investigated.

Keywords: RIA, nuclear fuel performance, thermomechanical calculations.

1. Introduction

The simulation, calculation and study of the fuel behaviour during RIA (Reactivity Initiated Accident) is very difficult and complex. Moreover, deep understanding of the RIA processes requires more and more experimental studies and tests of both fresh and irradiated fuel of different types in research reactors and another research facilities.

The RIA belongs to DBAs (Design Basis Accidents), specifically the case of control rod ejection in PWR (Pressurized Water Reactor). After control rod ejection, the fuel rod power increases rapidly but this increase is reduced by Doppler effect immediately. Thus, RIA scenario is well characterized by power peak and amplitude. In general, the RIA scenario can be divided into two phases. The first phase, early phase of transient or from the point of view of fuel often called PCMI (Pellet-Cladding Mechanical Interaction) phase, describes few first milliseconds of transient. The fuel power increase leads to prompt increase in fuel temperature, which further causes rapid thermal expansion of fuel. It is followed by closure of the gap in the case of fresh fuel or low burnup fuel (there is still gap between fuel and cladding before transient), because in this early phase of transient the temperature of cladding is still unchanged and relatively low (there is no or only small thermal expansion of cladding whereas the thermal expansion of pellets is due to high temperature of fuel faster and larger). On the contrary in the case of high burnup fuel, where the gap is already closed during normal operation, the rapid thermal expansion of the fuel can lead to failure of the "cold" cladding, this is called PCMI-failure. This scenario is schematically shown in Figure 1 on the left. For this type of failure the long axial crack is typical, Figure 2a.

The second phase of the transient is characterized by cladding temperature increase and therefore it is sometimes called high temperature phase. Description of fuel behaviour during this phase is similar to fuel bahaviour during LOCA (Loss of Coolant Accident). Due to temperature increase the FGR (Fission Gas Release) increases and this causes the increase of rod inner pressure. In some region the instability criterion can be exceeded which lead to cladding ballooning and the burst can follow. This scenario is shown in the middle in Figure 1. For the burst it is typical a short axial crack which can be seen in Figure 2b.

Another failure mode is characterized by radial crack or disruption of the cladding, it is shown in Figure 2c. If the energy received by fuel during transient is too high, it can lead to partially melting of fuel and also of cladding. This type of crack is also typical for the post transient failure caused by thermal shock after re-wetting.

Currently, there is an ongoing programme called HERA with the goal of understanding LWR (Light Water Reactor) fuel performance at high burnup under RIA condition. Another partial goals are to quantify the impact of pulse width on fuel performance, obtain new data on high burnup fuel under pulse conditions, quantify the additional margin provided by modern cladding alloys to PCMI failure limits and offer improved data for modelers using specially designed tests that eliminate key uncertainties in high-burnup fuel tests [2]. The facilities, that house HERA programme, are TREAT (Transient Reactor Test Facility) reactor and hot cells in Idaho (USA) [3, 4] and NSRR (Nuclear

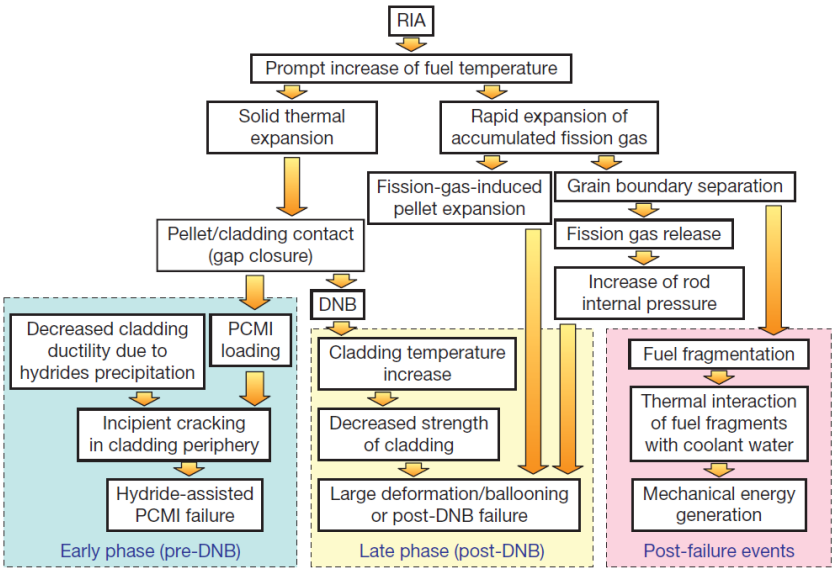

Figure 1. Schematic drawing of fuel rod processes during RIA [1].

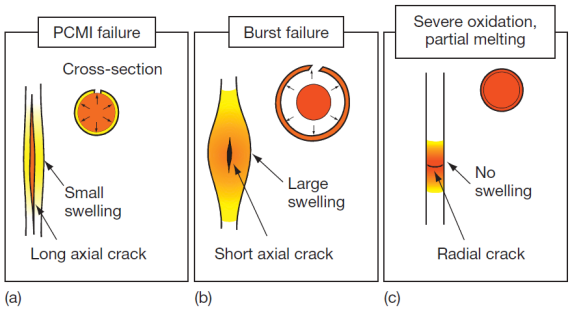

Figure 2. Schematic drawing of three possibilities of failure [1].

Specimen parameter	TREAT	NSRR
Fuel	Fresh UO_2	
Cladding	Zry-4 (SRA)	
Fuel Pellet Height [mm]	10.160	
Number of Pellets	10	12
Total Fuel Mass [g]	57.9	69.4
Cladding Inner Radius [mm]	4.1785	
Cladding Outer Radius [mm]	4.7500	
Plenum Pressure [MPa]	0.1	
Rod Free Volume [cm^3]	1.23	2.52
Water Temperature [°C]	20	
Capsule Pressure [MPa]	0.1	

Table 1. Specimen and setup parameters for both TREAT and NSRR facilities.

Safety Research Reactor) reactor in Japan [5].

Except of the experimental part, there is also modelling and simulation task included in HERA programme. In this part many organisations with many codes are involved. The description of the calculation provided in FRAPTRAN thermomechanical code at the CTU (Czech Technical University) is presented in the following text.

2. Modelling and simulation

The parameters and the geometry of the calculated cases were given by the HERA programme leaders. The simulated geometry copies the geometry and ambient conditions of both experimental facilities (TREAT and NSRR) as close as possible. Then there was built the calculation matrix, which should show the effects of chosen parameters (pulse width, hydrogen content, enthalpy increase and gap size) of the fuel performance during transient conditions and which is described later in this chapter.

2.1. Geometry of the design experiments

As mentioned above, the geometry in a simulation was dimensionally identical to an experimental one. The test specimen was based on a fresh 17×17 PWR type fuel design in all cases. The Zry-4 cladding and UO_2 fuel, typical for LWR were used. During the experiments the fuel was surrounded by stagnant water at room temperature and under normal pressure. In general, there were two types of specimens, because there were two types of experimental facilities (TREAT and NSRR). The exact parameters and differences between this two experimental setups are provided in Table 1 [6].

The Figure 3 shows the simplified schema of the capsule. The rodlet is placed in the centre of the capsule, the capsule is partially filled with water and the rest of the capsule volume is filled with argon. The specification of the capsule parameters for both TREAT and NSRR capsule are in Table 2. These parameters represent basic hydraulic information. In general, there are two basic possibilities how the boundary (hydraulic) conditions can be solved in thermomechanical calculations. Firstly, the cooling can be solved by system code and results act as a boundary condition in subsequent thermomechanical code. And the second

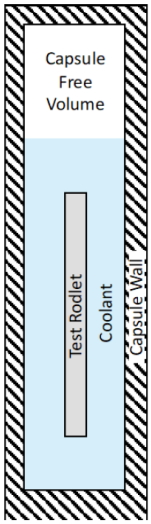

FIGURE 3. Schematic drawing of th capsule of experimental setups [6].

Capsule parameter	TREAT	NSRR
Water Outer Radius [mm]	25	120
Water Volume [cm^3]	280	6250
Argon Free Volume [cm^3]	500	2350

TABLE 2. The specification of the capsule parameters – TREAT and NSRR facilities [6].

possibility is to have thermomechanical code which can solve thermohydraulic issues.

2.2. MATRIX OF THE CALCULATIONS

The simulations were focused on PCMI and the matrix of the calculation was designed to cover several effects (pulse width, enthalpy increase, hydrogen concentration and gap size). As mentioned before, the cladding can fail due to PCMI and one of the most important aspects of the cladding PCMI failure is the value of hydrogen concentration in cladding material. The higher hydrogen content has a negative effect of cladding failure resistance, especially during PCMI. The cracks start to form in the brittle hydride rim and then propagate through the metallic substrate. It is obvious that the forming of hydride rim and the width of hydride rim grows with the increasing hydrogen content in cladding.

Temperature of cladding is another very important parameter which influences fuel behaviour during PCMI. Thermal expansion and creep rate of cladding increases with temperature and thus the load of the cladding from fuel pellet during PCMI is smaller at higher temperatures. The temperature of the cladding during early phase of RIA can be affected by pulse width in a way that wider pulses lead to high temperature of cladding. Therefore, the probability of failure during PCMI is higher when the pulse is narrower with the assumption of the same energy.

Of course, gap size is another parameter affecting

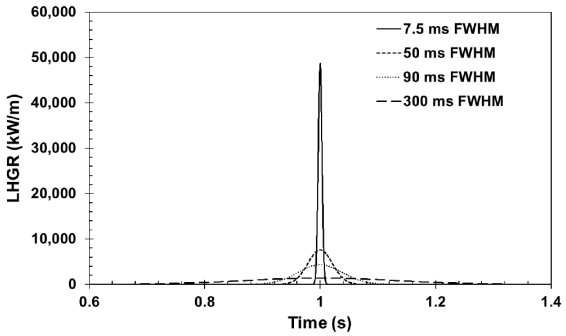

FIGURE 4. Power distributions for four pulse widths [6].

the probability of PCMI failure. In the case of smaller gap, there is small space where the pellet can expand due to thermal expansion and the loading of the cladding increases. On the other hand, the heat transfer decreases with increase of gap size.

Last mentioned parameter affecting the PCMI phenomena is enthalpy increase or inserted energy. If the enthalpy increase, the cladding vulnerability to failure during PCMI or whole RIA transient gets bigger.

The above mentioned phenomena are the most important effects influencing PCMI or early phase of RIA. The matrix of calculations considers all these effects and includes 14 sets of parameters. The matrix can be seen in Table 3. There are two different gap size values: 18 µm and 48 µm, three hydrogen content values: 400 ppm (to which hydride rim thickness of 80 µm corresponds), 200 ppm (40 µm) and 600 ppm (140 µm), three enthalpy increase values: 650 J/g, 550 J/g and 750 J/g and four pulse width at FWHM (Full Width Half Maximum) values: 7.5 ms, 90 ms, 50 ms and 300 ms, where pulse width value of 7.5 ms corresponds to the test facility in NSRR and the other values of pulse width correspond to the facility in TREAT. The linear heat generation rate (LHGR) versus time for four pulse width variations are shown in Figure 4. The pure Gaussian temporal profile is assumed for power input.

2.3. FRAPTRAN

FRAPTRAN (The Fuel Rod Analysis Program Transient) is thermomechanical Fortran language computer code. FRAPTRAN models and calculations are focused on fuel behaviour in LWR, especially during transients and accidents such as LOCA and RIA. In general, FRAPTRAN computes the temperature and deformation dependence on time of the fuel rod. FRAPTRAN can be used alone or with the initialization from the FRAPCON (steady state fuel performance code). The main phenomena simulated by FRAPTRAN are heat conduction in fuel rod and heat transfer from cladding to coolant, elastic-plastic deformation of fuel and cladding, FGR, fuel rod gas pressure and cladding oxidation.

The input parameters are time-dependent fuel rod power and coolant boundary conditions with several

Case	Facility	Pulse Width at FWHM [ms]	Peak Radial Average Enthalpy Increase [J/g]	Hydrogen Content/Rim thickness [ppm/µm]	Fuel Outer Radius [mm]
1	NSRR	7.5	650	400/80	4.1605
2	NSRR	7.5	650	200/40	4.1605
3	NSRR	7.5	650	600/140	4.1605
4	NSRR	7.5	550	400/80	4.1605
5	NSRR	7.5	750	400/80	4.1605
13	NSRR	7.5	650	400/80	4.1305
6	TREAT	90	650	400/80	4.1605
7	TREAT	90	650	200/40	4.1605
8	TREAT	90	650	600/140	4.1605
9	TREAT	90	550	400/80	4.1605
10	TREAT	90	750	400/80	4.1605
14	TREAT	90	650	400/80	4.1305
11	TREAT	50	650	400/80	4.1605
12	TREAT	300	650	400/80	4.1605

Table 3. Case matrix

ways how to calculate and simulate boundary conditions. The first one is labelled as "coolant" option in input file. If the user chooses this option, the boundary conditions are calculated by FRAPTRAN, where nucleate boiling heat transfer, critical heat flux (CHF) and post-CHF heat transfer correlations are included in thermohydraulic model. In this case the coolant pressure, temperature and mass flux have to be entered by user to the input file and the geometry of the coolant channel has to be specified. User can choose from different nucleate boiling heat transfer, CHF and post-CHF heat transfer correlations but the default setting is following: Dittus-Boelter correlation for nucleate boiling heat transfer, EPRI-1 correlation for CHF and modified Tong-Young and Groeneveld 5.9 correlations for transition and film boiling.

The second way how to obtain boundary conditions is called "heat" option in the input file. This way is mainly used in the case that the cladding temperature is known, i.e., the temperature is measured by thermocouples during experiment or the temperature history is calculated by specialized thermohydraulic code (mainly system codes) [7].

3. Discussion and results

There are several parameters which were observed to compare results of all cases, the most important are failure prediction (from the point of view of all observed effects), cladding outer surface temperature (comparison of used thermohydraulic approach) and stress intensity factor, which was defined by the following relation:

$$SIF = \sigma_\Theta \cdot \sqrt{\pi a}. \quad (1)$$

where a is the crack length which was assumed to be equal to the thickness of the hydride rim, and σ_Θ is hoop stress. This parameter takes stress field in the cladding and hydride rim into account. There were far more parameters (fuel centreline temperature, hoop and axial strain, elongation, inner rod pressure, ...) monitored but only some will be evaluated here.

The rod power histories, which represent input parameters, were design in order to the centre of power peak was at the time of 1 second. And the whole simulation was 200 seconds long.

3.1. Boundary conditions setting effect

As was explained above there are mainly two possibilities how to obtain boundary conditions, which means cladding outer temperature in this case. First way is using boundary conditions calculated by system code RELAP [8] by the leaders of the HERA programme. This data should be relatively accurate because it was calculated by specialized thermohydraulic code. The second way how to calculate boundary condition is using FRAPTRAN thermohydraulic model.

The comparison of cladding outer temperature calculated with two different approach is shown in Figure 5 for the cases 1, 6, 11 a 12. It is shown that the difference between these two calculations is enormous. Low cladding temperature and fast decrease of temperature in the calculation by FRAPTRAN is caused by inadequate thermohydraulic model for this type of cooling and experimental setup. There is a brief moment when both calculation approaches result in similar temperature values (especially in the cases with narrower power peaks) and it is time interval from the start of calculation (t = 0 seconds) to the time of about 1.02 seconds. In this interval the differences between both approaches are negligible. This observation implies that when the target of interest is PCMI phenomena (these phenomena occur in the early stage of transient) both approaches are inter-

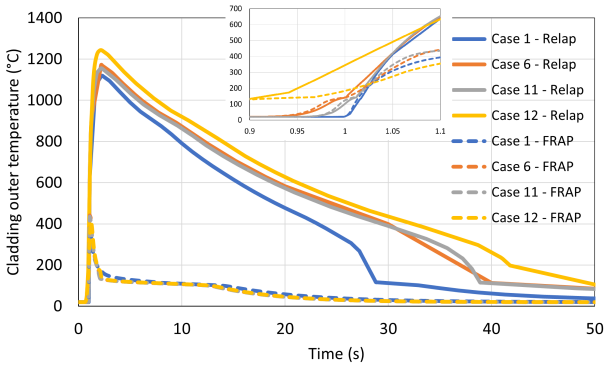

FIGURE 5. Cladding outer temperature versus time in cases 1, 6, 11 a 12 and comparison two ways of calculating boundary conditions: full line represents RELAP temperature results and dash line represents results from FRAPTRAN thermohydraulic model.

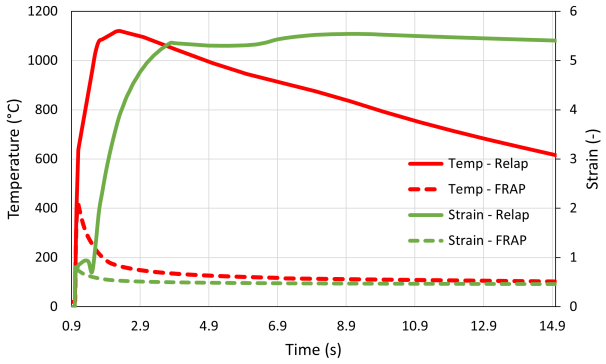

FIGURE 6. Case 13: Cladding outer temperature and strain with the both types of boundary conditions – calculated by RELAP and by FRAPTRAN thermohydraulic model.

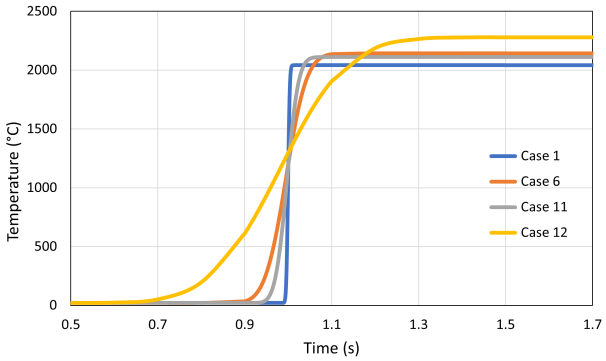

FIGURE 7. Time dependence of fuel centre temperature for four cases with different pulse width (case 1 – 7.5 ms, case 6 – 90 ms, case 11 – 50 ms and case 12 – 300 ms).

changeable and they should have similar results of fuel behaviour.

It is also interesting to compare the results of failure prediction versus boundary condition effect. For example, the case 1, the simulation using RELAP boundary conditions predicted no failure, whereas the calculation using FRAPTRAN thermohydraulic model predicted failure of the rod at the time of 1.006 seconds. Another case is shown in the graph in Figure 5, the case 12 calculation using FRAPTRAN model predicted no failure of rod, on the other hand the simulation using RELAP cladding temperature predicted rod failure at time of 31 seconds with the initialization of cladding ballooning at the time of 3.4 seconds.

Another example how failure prediction can be influence by calculation of boundary condition is shown in the graph in Figure 6. In the graph the results of the calculation of case 13 (NSRR, 7.5 ms, 650 J/g, 400 ppm, 4.1305 mm of fuel radius) is shown, again it is possible to see the difference in cladding outer temperature (shown in red) between both ways of determining boundary condition. From that difference the different failure prediction follows. The first calculation with FRAPTRAN boundary condition predicted no failure, whereas in the second calculation with RELAP boundary condition there was predicted rod failure due to ballooning and following burst after 23 seconds from the beginning of the calculation. The green curves in the graphs show the strain history and again big difference in both approaches is observed.

3.2. Pulse width effect

There were four different pulse widths in the case matrix: 7.5 ms, 50 ms, 90 ms and 300 ms. Firstly, the difference in temperature history can be seen in the graphs (cladding temperature – Figure 5, fuel temperature – Figure 7, the results with RELAP boundary conditions are presented here), the first increase of temperature was in case 12, i.e. with the widest pulse and in the same case the temperature reached the highest point. The same observation was in both cladding and fuel temperature. In the graph in Figure 7 a little bit different fuel temperature history can be seen, with the comparison with cladding temperature history, the fuel temperature in case 1 (narrower pulse) starts increasing as the last (from investigated cases) but then the increase is very fast and steep, thus the maximum fuel temperature in this case is reached first (from investigated cases). On the other hand, the temperature increase by the case 12 (widest pulse) is not so steep and the maximum temperature is reached later.

The effect of pulse width can be seen from the results of cladding hoop stress. In the graph in Figure 8 time dependence of hoop stress is shown. The stress peak slightly follows the power peak shape. For example, the stress peak in the case 1 (the narrowest and the highest power peak) is the narrowest and highest.

3.3. Enthalpy increase effect

The time-dependent enthalpy and the total energy deposited per unit mass of fuel is shown in the graph in Figure 9 for cases 6, 9 and 10. The influence of enthalpy increase can be shown also in temperature history in the graph in Figure 10. As it was expected, the highest temperature is in the case of the highest

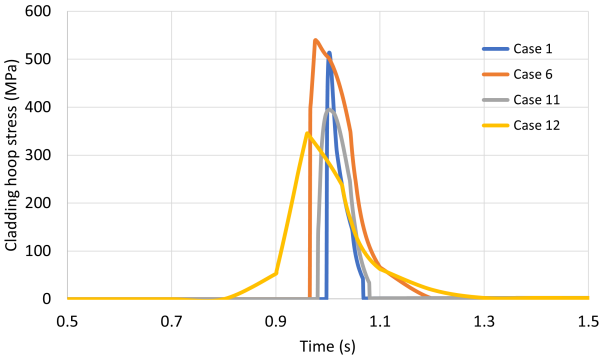

Figure 8. Time dependence of cladding hoop stress for four cases with different pulse width (case 1 – 7.5 ms, case 6 – 90 ms, case 11 – 50 ms and case 12 – 300 ms).

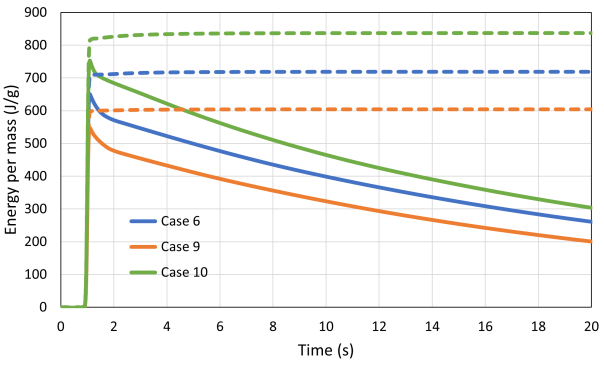

Figure 9. Time dependence of enthalpy increase and total energy deposited per unit mass of fuel for three cases with different enthalpy increase (case 6 – 650 J/g, case 9 – 550 J/g and case 10 – 750 J/g).

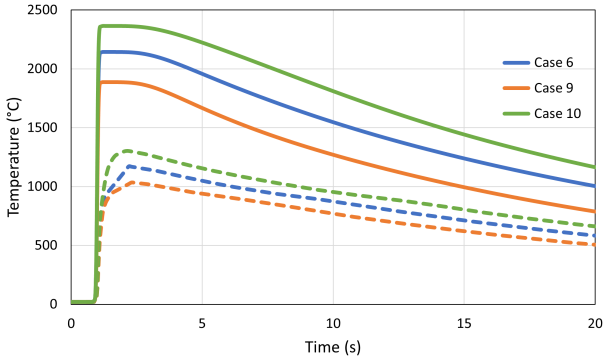

Figure 10. Time dependence of fuel centreline temperature (full line) and cladding outer temperature (dashed line) for three cases with different enthalpy increase (case 6 – 650 J/g, case 9 – 550 J/g and case 10 – 750 J/g).

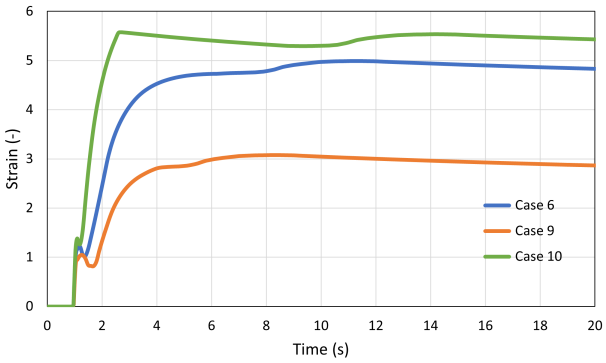

Figure 11. Time dependence of cladding hoop strain for three cases with different enthalpy increase (case 6 – 650 J/g, case 9 – 550 J/g and case 10 – 750 J/g).

enthalpy increase, i.e., case 10 with enthalpy increase of 750 J/g.

The difference between these three cases can be seen also in the strain history, for example between cases 6 and 9 (650 and 550 J/g). The hoop strain in the case 6 is about twice as big as the hoop strain in the case 9, the strain history for all three cases can be seen in the graph in Figure 11.

The strain is then connected with the failure prediction. In the case 10 the rod failure was supposed by code, more precisely at time of 33 seconds and at time of 2.7 second the cladding ballooning initialization was predicted (the time can be seen in the graph in Figure 11 it is the sharp change of the green curve, because the ballooning model was shut down thus there is no larger deformation calculated). In the other two cases (6 and 9) no rod failure was predicted.

3.4. Hydrogen effect

The hydrogen effect is evident, the embrittlement of cladding increases with increasing hydrogen content and following formation of hydrides. But modelling the hydrogen content and its effect on fuel behaviour is more complicated and there are only a few codes which can solve and assume the influence of hydrogen content on fuel performance. In FRAPTRAN there is possibility to set hydrogen content, but the influence on results is very limited. The input of hydrogen content is used only in the low-temperature PCMI cladding failure model and it is assumed that hydrogen content is uniformly and homogenously distributed. In other models the hydrogen content is not assumed, so the influence of hydrogen content on other parameters (stress, strain, deformation) is neglected in the code, although in the reality they are affected by hydrogen content.

The hydrogen effect can be seen for example in the cases 1-3, the only difference between these cases is in the value of hydrogen content (case 1 – 400 ppm, 2 – 200 ppm and 3 – 600 ppm). The rod failure was predicted only in case 3 and the histories of all parameters were the same until rod failure in this case. Due to higher hydrogen concentration in case 3 the failure strain was the lowest one and the hoop strain exceeded it, thus the rod failure at time of 1.003 seconds was predicted by code in case 3.

The similar approach is in the calculation of hydride rim, there are only few codes which assume and calculate formation and effect of hydride rim. In the FRAPTRAN models the hydride rim is not calculated. In this case the effect of hydride rim can be considered only in the calculations of SIF parameter

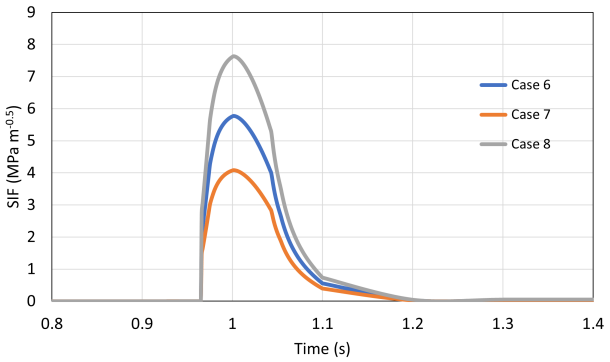

FIGURE 12. Time dependence of SIF (Stress Intensity Factor) for three cases with different hydrogen content and hydride rim size (case 6 – 400 ppm/80 µm, case 7 – 200 ppm/40 µm and case 8 – 600 ppm/140 µm).

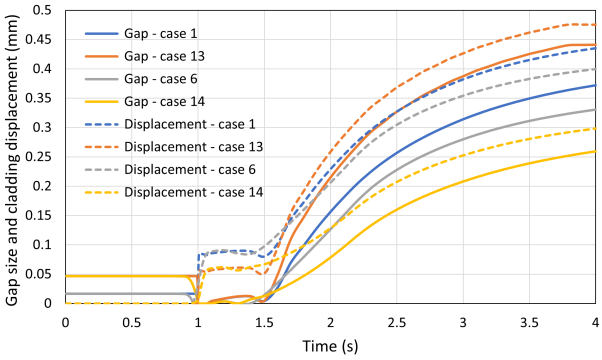

FIGURE 13. Time dependence of gap size and cladding hoop displacement for four different cases (case 1 and 6 – fuel radius of 4.1605 mm and case 13 and 14 – fuel radius of 4.1305 mm).

(Equation (1)) which follow the FRAPTRAN stress calculation. SIF parameter can be than used for prediction of failure if the SIF exceeds some critical value. The influence of width of hydride rim on SIF can be seen in graph in Figure 12.

3.5. GAP SIZE EFFECT

The gap size effect of fuel behaviour during early phase of RIA, especially the influence of this effect on PCMI phenomena is obvious. If the gap is narrower, there is less space for fuel thermal expansion which leads to bigger hoop stress of cladding. This can be seen from the comparison of calculations of case 1 and case 13 (using FRAPTRAN boundary conditions). Only difference in these cases is in geometry of gap (fuel pellet diameter, case 1 – 8.321 mm, case 13 – 8.261 mm). During the case 1 calculation the rod failure was predicted by code, whereas in case 13 there was no predicted failure.

On the other hand, the vulnerability of cladding to failure in the second high temperature phase of RIA is higher if the gap is wider. With the increasing gap size fuel temperature increases and the fuel thermal expansion is bigger, this is caused by decrease of thermal conductivity. The increasing temperature leads to larger FGR which then leads to increase of rod inner pressure and increase of hoop cladding stress and strain. If strain exceed the instability criterion the rod tends to balloon and it can lead to rod burst. An example can be seen from the comparison of case 1 and 13 with use RELAP boundary condition. In case 13 the rod failure (due to ballooning and burst) was predicted by code, unlike case 1 where no failure was predicted. The gap size and cladding displacement history is shown in Figure 13.

4. CONCLUSIONS

To sum up the results, 14 calculations for two types of boundary conditions (total 28) were provided. Influence of four effects (pulse width, enthalpy increase, hydrogen content and gap size) on the fuel performance was investigated within the HERA programme modelling and simulation task.

Increasing pulse width causes higher maximum cladding and fuel temperatures which lead to larger strains. On the other hand, cladding hoop stress decreases with the increasing pulse width. Similar dependence can be seen in enthalpy increase effect, with the increasing energy the cladding and fuel temperature increase and hoop deformation decreases. Thus, the fuel rod is more vulnerable to failure during larger enthalpy increases.

Also, the increasing hydrogen concentration makes the rod more vulnerable to failure and the embrittlement of cladding is bigger. This expected phenomenon can be only limitedly modelled by FRAPTRAN, because hydrogen content is considered only in low-temperature PCMI cladding failure model. The creation and size of hydride rim is not assumed in FRAPTRAN.

Then, the gap size plays an important role in the fuel rod performance in both improving or worsening of the fuel performance. If the gap is bigger there is more space for fuel thermal expansion and bigger margin to PCMI failure, on the other hand the bigger gap adversely impacts heat transfer and fuel temperature. And as was shown above, this phenomenon can lead to cladding failure due to ballooning and burst.

In addition to HERA programme the investigation of influence of boundary condition was provided. Two ways how to obtain boundary conditions are described in this paper - using specialized thermohydraulic code RELAP and using FRAPTRAN thermohydraulic model. It was shown that the difference is significant with the exception of very early stage of transient, thus the PCMI phenomena can be evaluated by using both of these approaches with similar level of accuracy. The differences can be caused by limitations of thermohydraulic model in FRAPTRAN which is intended for the cases with forced circulation in default, so the calculation with mass flux of zero is significantly unstable and so the calculation of stagnant water condition is more complicated.

The more precisely calculation of boundary conditions should be developed in the future work, for example, some analysis using different setting of thermo-hydraulic model in FRAPTRAN should be computed. And then there should be also focus on modelling of phenomena whose simulation was neglected or simplified here, e.g., higher hydrogen concentration in the outer periphery of cladding or implementation of another failure criterion.

References

[1] T. Fuketa. 2.22 – transient response of LWR fuels (RIA). In R. J. Konings (ed.), *Comprehensive Nuclear Materials*, pp. 579–593. Elsevier, Oxford, 2012. https://doi.org/10.1016/B978-0-08-056033-5.00044-6

[2] High-burnup Experiments in Reactivity Initiated Accidents (HERA), 2022.

[3] C. L. Pope, C. B. Jensen, D. M. Gerstner, J. R. Parry. Transient reactor test (TREAT) facility design and experiment capability. *Nuclear Technology* **205**(10):1378–1386, 2019. https://doi.org/10.1080/00295450.2019.1599615

[4] B. Heath, C. Jensen. Thermal design of the TREAT facility. *Nuclear Technology* **206**(9):1436–1448, 2020. https://doi.org/10.1080/00295450.2020.1725370

[5] T. Mihara, Y. Udagawa, M. Amaya. Experimental capability of Nuclear Safety Research Reactor (NSRR), 2017.

[6] C. Jensen, D. Kamerman, C. Folsom, S. Seo. HERA M & S Exercise Problem Description Report, 2023.

[7] K. Geelhood, W. G. Luscher, J. M. Cuta, I. E. Porter. FRAPTRAN-2.0: A computer code for the transient analysis of oxide fuel rods. Tech. rep., Pacific Northwest National Laboratory, 2016.

[8] RELAP5/MOD3 Code Manual: User's Guide and Input Requirements, 1995.